



MATHEMATICAL MODELLING OF CREEP TRANSITION IN STRUCTURAL COMPONENTS COMPOSED OF TITANATE CERAMICS FABRICATED AS ANNULAR ROTATING DISCS
MATEMATIČKO MODELIRANJE PRELAZNIH NAPONA PUZANJA U KOMPONENTAMA KONSTRUKCIJA PRSTENASTIH ROTIRAJUĆIHH DISKOVA OD TITANAT KERAMIKE

Originalni naučni rad / Original scientific paper
Rad primljen / Paper received: 12.10.2022
<https://doi.org/10.69644/ivk-2024-03-0323>

Adresa autora / Author's address:
¹⁾ DCA, CCT, Chandigarh Group of Colleges, India S. Shahi 
0000-0002-4991-3164 *email: shivdevshahi93@gmail.com
²⁾ UILS, Chandigarh University, India G. Kaur  0000-0003-1903-5994

Keywords

- creep
- disc
- ceramics
- stresses
- strains

Abstract

Analytical characterization of creep stresses and strains in annular ceramic discs experiencing high centrifugal forces is of much significance in the theory of structural components. In this paper transition theory has been incorporated to obtain these stresses and strains in ceramic discs which exhibit transversely isotropic macro structural symmetry and having a bore at the centre on which it rotates. Yield criteria from the classical theory are not assumed for the analysis. The creep transition stresses are obtained by transition theory. The analytical solution is applied on ceramic discs. Stiffness constants are obtained by ultrasonic wave propagation method. Analytical solution results are plotted graphically. It is observed that the centrifugal forces increase the magnitude of radial and circumferential stresses at the internal surface of discs. Strains are maximal at internal surface and diminish toward the outer surface. The rise in strains proportional to increasing angular speed infers to the fact that the disc will tend to fracture at the bore adjoining the inclusion when subjected to higher centrifugal forces.

INTRODUCTION

Ceramic discs are characterised by chemical inertness, high melting point, low electrical and thermal conductivity. Traditional ceramics include insulating materials, glass, abrasives and enamels. In the present times, as typical examples, thermal and electrical insulations for various structural components are manufactured using ceramics as a base. Ceramic discs are presently being extensively used in the manufacture of capacitors, filtration discs, automobile braking systems, gas turbines, etc. A material is said to exhibit transverse isotropy when physical properties for that material are alike in a single preferential direction. This particular property provides an edge in the manufacture of thin structural components under state of plane stress. Creep strains of such materials are accompanied by changes in their structure which are irreversible. Creep analysis of such dynamic structural components is necessary for predetermining their deformation, fracture points and for stable design. In this paper, we examine creep deformation of annular ceramic discs

Ključne reči

- puzanje
- disk
- keramika
- naponi
- deformacije

Izvod

Analička karakterizacija napona i deformacija puzanja u prstenastim keramičkim diskovima koji su izloženi visokim centrifugalnim silama je od velikog značaja u teoriji konstrukcija komponenata. U radu je primenjena teorija prelaznih napona za proračun ovih napona i deformacija u keramičkim diskovima koji ispoljavaju poprečnu izotropnu makro strukturu simetriju sa provrtom u centru rotacije. U analizi nisu pretpostavljeni kriterijumi tečenja iz klasične teorije. Prelazni naponi puzanja dobijeni su teorijom prelaznih napona. Analitičko rešenje se izvodi za keramičke diskove. Konstante krutosti su dobijene metodom prostiranja ultrazvučnog talasa. Rezultati analitičkog rešenja su prikazani grafički. Uočeno je da centrifugalne sile povećavaju radijalne i cirkularne napone na unutrašnjoj površini diska. Deformacije su maksimalne na unutrašnjoj površini i smanjuju se ka spoljnoj površini. Povećanje deformacija, koje je proporcionalno porastu ugaone brzine, upućuje na činjenicu da disk ima tendenciju loma na provrtu u okolini uključka pri većim centrifugalnim silama.

experiencing high centrifugal forces and transversely isotropic macro-structural symmetry. Numerical values of elastic stiffness constants for two ceramic materials have been used to calculate the trends of creep stresses and strains. The centrifugal forces are added to the analysis by altering the equation of equilibrium accordingly. Wang and Cao /25/ determined the elastic constants of lead zirconate titanate (PZT-5H) using ultrasonic wave propagation. Elastic constants for barium titanate are given by Royer and Dieulesaint /11/.

The analysis for structures made of monolithic materials, composites, functionally graded materials, exhibiting the respective isotropy and anisotropy are given in most standard textbooks /1-3, 7-10, 17, 23-24/. Transition is a naturally occurring phenomenon nonlinear in character. Creep analysis assumes certain ad hoc assumptions like incompressibility and yield criterion, which is insufficient to analyse the transition phase. Seth's transition theory /12, 13/ bypasses these assumptions. The generalised principal strain measure was first defined by B.R. Seth, /12/:

$$e_{ii} = \int_0^A \left[1 - 2e_{ii}^A\right]^{\frac{n}{2}-1} d e_{ii} = \frac{1}{n} \left[1 - (1 - 2e_{ii}^A)^{\frac{n}{2}}\right], \quad (1)$$

where: $i = 1, 2, 3$.

The theory has been used to solve various problems of transitional stress and strain determination in structures modelled in the form of discs exhibiting transverse isotropy and orthotropy, /4-6, 14, 15, 18-22, 26/.

GOVERNING EQUATIONS

Ceramic annular disc having a perforation of thickness a and external radius b is modelled. This ceramic disc is experiencing high centrifugal forces in the radial direction. There is no variation in the density and thickness of the ceramic disc. The axial stresses will not be considered in this case due to plane stress conditions. The displacement components are given as:

$$u = r(1 - \beta), \quad v = 0, \quad w = dz, \quad (2)$$

where: β is a function depending on radius only.

The generalised strain component given by Seth /12/ is represented as:

$$e_{rr} = -\left[(\beta + r\beta')^n - 1\right], \quad e_{\theta\theta} = -[\beta^n - 1],$$

$$e_{zz} = -\left[(1-d)^n - 1\right], \quad e_{r\theta} = e_{\theta z} = e_{zr} = 0.$$

Considering $n = 1$ as the measure and

$$\beta' = d\beta / dr. \quad (3)$$

For materials exhibiting transverse isotropy, following relations of stress-strain have been defined, /17/:

$$T_{rr} = C_{11}e_{rr} + C_{13}e_{zz} + (C_{11} - 2C_{66})e_{\theta\theta},$$

$$T_{\theta\theta} = C_{11}e_{\theta\theta} + C_{13}e_{zz} + (C_{11} - 2C_{66})e_{rr},$$

$$T_{zz} = C_{13}e_{rr} + C_{33}e_{zz} + C_{13}e_{\theta\theta} = 0,$$

$$T_{zr} = T_{\theta z} = T_{r\theta} = 0. \quad (4)$$

The strain components are obtained in terms of radial and circumferential stresses from Eqs. (4) and (3):

$$e_{rr} \equiv \frac{\partial u}{\partial r} - \frac{1}{2} \left(\frac{\partial u}{\partial r} \right)^2 = \frac{1}{2} [1 - (r\beta' + \beta)^2] =$$

$$= \frac{1}{E} \left[T_{rr} - \left(\frac{C_{11}C_{33} - C_{13}^2 - 2C_{66}C_{33}}{C_{11}C_{33} - C_{13}^2} \right) T_{\theta\theta} \right],$$

$$e_{\theta\theta} \equiv \frac{u}{r} - \frac{u^2}{2r^2} = \frac{1}{2} [1 - \beta^2] =$$

$$= \frac{1}{E} \left[T_{\theta\theta} - \left(\frac{C_{11}C_{33} - C_{13}^2 - 2C_{66}C_{33}}{C_{11}C_{33} - C_{13}^2} \right) T_{rr} \right],$$

$$e_{zz} \equiv \frac{\partial w}{\partial z} - \frac{1}{2} \left(\frac{\partial w}{\partial z} \right)^2 = \frac{1}{2} [1 - (1-d)^2] =$$

$$= -\frac{1}{E} \left(\frac{C_{11}C_{33} - C_{13}^2 - 2C_{66}C_{33}}{C_{11}C_{33} - C_{13}^2} \right) [T_{rr} - T_{\theta\theta}],$$

$$e_{r\theta} = e_{\theta z} = e_{zr} = 0, \quad (5)$$

where: T_{rr} and $T_{\theta\theta}$ are the principal stresses,

$$E = 4C_{66} \left(\frac{C_{11}C_{33} - C_{13}^2 - C_{66}C_{33}}{C_{11}C_{33} - C_{13}^2} \right),$$

where: E is Young's modulus of elasticity.

Substituting Eqs.(4) into Eqs.(5), we get:

$$T_{rr} = -\frac{2C_{66}}{n} [1 - \beta^n] + \frac{A}{n} [2 - \beta^n (1 + [1 + P]^n)],$$

$$T_{\theta\theta} = -\frac{2C_{66}}{n} [1 - \beta^n [1 + P]^n] + \frac{A}{n} [2 - \beta^n (1 + [1 + P]^n)],$$

$$T_{zz} = T_{r\theta} = 0, \quad T_{zr} = T_{\theta z} = 0, \quad (6)$$

for $A = C_{11} - (C_{12}^2/C_{33})$.

The required equation of equilibrium for ceramic disc is given as:

$$\frac{d}{dr} (rT_{rr}) - T_{\theta\theta} + \rho\omega^2 r^2 = 0. \quad (7)$$

The boundary conditions at internal and external radius are given as:

at internal radius $r = a$, displacement $u = 0$
 at external radius $r = b$, radial stress $T_{rr} = 0$. (8)

From Eqs. (6) and (7), we get the following nonlinear differential equation:

$$\frac{\rho\omega^2 r^2}{A} + \beta^n \left[\frac{2C_{66}}{nA} (1 + nP - [1 + P]^n - P[1 + [1 + P]^n]) \right] =$$

$$= \beta^{n+1} [1 + P]^{n-1} \frac{dP}{d\beta}, \quad (9)$$

where: $r\beta' = \beta P$ (P is function of β , and β is function of r only).

Transition points of β in Eq.(9) are $P \rightarrow -1$ and $P \rightarrow \pm\infty$.

Solution for creep stresses through difference of principal stresses

The transition function \mathbb{C} is obtained through the difference of radial and circumferential stresses /5, 6, 16/. Creep stresses are obtained from the transition point $P \rightarrow -1$,

$$\mathbb{C} \equiv T_{rr} - T_{\theta\theta} = \frac{2C_{66}\beta^n}{n} [1 - [1 + P]^n]. \quad (10)$$

Taking the logarithmic differentiation and substituting the value of $dP/d\beta$ from Eq.(9) in Eq.(10), we get:

$$\frac{d}{dr} (\log \mathbb{C}) \equiv -\frac{1}{r} \left(-2n - \frac{n\rho\omega^2 r^2}{A\beta^n} + C_T(n-1) \right), \quad (11)$$

for $C_T = 2C_{66}/A$.

The asymptotic value of Eq.(11) at $P \rightarrow -1$ gives

$$\mathbb{C}(\text{principle stress difference}) = A_1 r^\eta \exp(\xi), \quad (12)$$

where: $\xi = -n\rho\omega^2 r^{n+2}/AD^n(n+2)$; $\eta = -2n + C_T(n-1)$.

From Eq.(12) and Eq.(8), we get:

$$T_{rr} = A_2 - A_1 \int r^{\eta-1} \exp(\xi) dr - \frac{\rho\omega^2 r^2}{2}, \quad (13)$$

where: A_1 and A_2 are constants which depend on the boundary conditions.

From boundary condition Eq.(8) and Eq.(13), we get

$$A_2 = A_1 \int_{r=b}^b r^{\eta-1} \exp(\xi) dr - \frac{\rho\omega^2 b^2}{2}. \quad (14)$$

Substituting Eq.(14) in Eq.(13), the radial stresses are given as:

$$T_{rr} = A_1 \int_r^b r^{\eta-1} \exp(\xi) dr + \frac{\rho\omega^2 (b^2 - r^2)}{2}. \quad (15)$$

From Eqs. (12) and (15), the circumferential stresses are given as:

$$T_{\theta\theta} = A_1 \left[\int_r^b r^{\eta-1} \exp(\xi) dr - r^\eta \exp(\xi) \right] + \frac{\rho\omega^2 (b^2 - r^2)}{2}. \quad (16)$$

Taking asymptotic value $P \rightarrow -1$ for Eq.(10),

$$\beta = \left(\frac{(T_{rr} - T_{\theta\theta})^n}{2C_{66}} \right)^{1/n} \Rightarrow \beta = \left(\frac{[A_1 r^n \exp(\xi)]^n}{2C_{66}} \right)^{1/n}. \quad (17)$$

From Eq.(17) and Eq.(2), the displacement is given as:

$$u = r - r \left(\frac{[A_1 r^n \exp(\xi)]^n}{2C_{66}} \right)^{1/n}, \quad (18)$$

where: $A_1 = 2C_{66}/na^{\eta-1}\exp(\xi_1)$; and $\xi_1 = -n\rho\omega^2 a^{n+2}/AD^n(n+2)$.

Principal stresses and displacement are obtained substituting A_1 in Eqs. (15), (16), and (18), respectively:

$$T_{rr} = \frac{2C_{66}}{na^\eta \exp(\xi_1)} \int_r^b r^{\eta-1} \exp(\xi) dr + \frac{\rho\omega^2 (b^2 - r^2)}{2}, \quad (19)$$

$$T_{\theta\theta} = \frac{2C_{66}}{na^\eta \exp(\xi_1)} \int_r^b r^{\eta-1} \exp(\xi) dr - r^\eta \exp(\xi) + \frac{\rho\omega^2 (b^2 - r^2)}{2}, \quad (20)$$

$$u = r - r \left(\frac{r^\eta \exp(\xi)}{a^\eta \exp(\xi_1)} \right)^{1/n}. \quad (21)$$

Conversion of principal creep stresses and displacement into non-dimensional components for generalizations $R = r/b$, $R_0 = a/b$, $\Omega^2 = r\omega^2 b^2/C_{66}$, $\sigma_r = T_{rr}/C_{66}$, $\sigma_\theta = T_{\theta\theta}/C_{66}$ and $u_1 = u/b$. Equations (19), (20), and (21) become:

$$\sigma_{rr} = \frac{2}{nR_0^\eta \exp(\xi_3)} \int_R^1 R^{\eta-1} \exp(\xi) dR + \frac{\Omega^2 (1 - R^2)}{2}, \quad (22)$$

$$\sigma_{\theta\theta} = \frac{2}{nR_0^\eta \exp(\xi_3)} \int_R^1 R^{\eta-1} \exp(\xi_2) dR - R^\eta \exp(\xi_2) + \frac{\Omega^2 (1 - R^2)}{2} \quad (23)$$

$$u_1 = R - R \left(\frac{R^\eta \exp(\xi_2)}{R_0^\eta \exp(\xi_3)} \right)^{1/n}, \quad (24)$$

where: $\xi_2 = -(n\Omega^2 R^{n+2}/2(n+2))(b/D)^n C_T$; and

$\xi_3 = -(n\Omega^2 R_0^2/2(n+2))(a/D)^n C_T$.

Solution for creep strains

The following relation is defined for stresses and strains in a disc:

$$e_{ij} = \left(\frac{A - 2C_{66}}{C_R} \right) \delta_{ij} T - \frac{2(A - C_{66})}{C_R} T_{ij}, \quad (25)$$

where: $C_R = 4C_{66}(C_{66} - A)$; and $A = C_{11} - C_{13}^2/C_{33}$.

From generalized strains we have

$$e_{\theta\theta} = -\beta^{n-1} \beta. \quad (26)$$

The Swainger measure defines $n = 1$, substituting it in Eq.(26) we get the relation

$$\dot{\epsilon}_{\theta\theta} = -\dot{\beta}. \quad (27)$$

We already have the transition value β ,

$$\beta = [T_{rr} - T_{\theta\theta}]^{1/n} [n/2C_{66}]^{1/n}. \quad (28)$$

From Eqs. (26), (27), and (28), we obtain the radial and circumferential strains as:

$$\dot{\epsilon}_{rr} = \frac{\left[1 - \frac{C_{13}^2}{C_{11}C_{33}} - 2 \frac{C_{66}}{C_{11}} \right] \sigma_{rr} - \left[1 - \frac{C_{13}^2}{C_{11}C_{33}} \right] \sigma_{\theta\theta}}{4 \left[\frac{C_{66}}{C_{11}} - 1 + \frac{C_{13}^2}{C_{11}C_{33}} \right]} \times \left[\frac{n}{2} (\sigma_{rr} - \sigma_{\theta\theta}) \right]^{n-1},$$

$$\dot{\epsilon}_{\theta\theta} = \frac{\left[1 - \frac{C_{13}^2}{C_{11}C_{33}} - 2 \frac{C_{66}}{C_{11}} \right] \sigma_{\theta\theta} - \left[1 - \frac{C_{13}^2}{C_{11}C_{33}} \right] \sigma_{rr}}{4 \left[\frac{C_{66}}{C_{11}} - 1 + \frac{C_{13}^2}{C_{11}C_{33}} \right]} \times \left[\frac{n}{2} (\sigma_{rr} - \sigma_{\theta\theta}) \right]^{n-1}. \quad (29)$$

Odqvist /10/ obtained similar results for principal creep stresses and strains.

NUMERICAL RESULTS AND DISCUSSION

Wang and Cao /25/ determined the elastic constants of lead zirconate titanate (PZT-5H) and characterized it to be a very useful piezoceramic. Elastic constants for barium titanate have been given by Royer and Dieulesaint, /11/. Graphs are plotted for creep stresses and displacement along the radii ratio $R = r/b$ for ceramic discs made of lead zirconate titanate (PZT-5H) and barium titanate exhibiting transversely isotropic symmetry in Figs. 1-6. The effect of centrifugal forces is observed by analysing the model at angular speeds $\Omega^2 = 50, 100, \text{ and } 150$. The variation in angular speed is shown in the proceeding figures. Radial stresses have maximal value at the inner surface of both the rotating disc, exhibiting transverse isotropy, and circumferential stresses decrease at the inner surface with increase in measure $n = 1/3, 1/5, \text{ and } 1/7$. It is also observed that centrifugal forces increase the magnitude of radial and circumferential stresses at the inner surface. This is observed for both types of ceramic discs. Similarly, strain rates have been calculated for both types of ceramic discs. The varying rates of strain with respect to changing angular speeds are represented in Figs. 7-12. Radial and circumferential strain rates clearly show that strain values are maximal at inner surfaces close to the bore and diminish along the outer surface. Both radial and circumferential strain rates show similar behaviour for

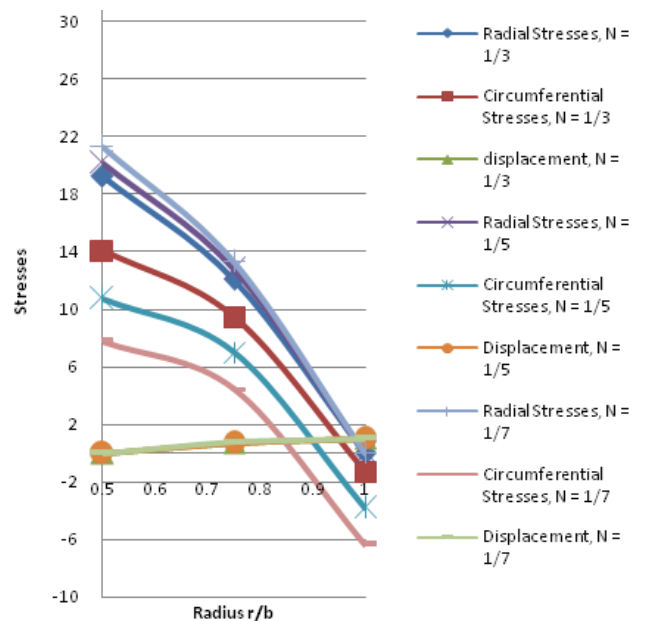


Figure 1. Creep stresses and displacement in PZT-5H along the radius ratios $R = r/b$ at $\Omega^2 = 50$.

the ceramic discs. It has also been observed that due to high intensity of stresses and strains close to the inner surface of the discs, the probability of damage to the disc close to the bore is higher.

CONCLUSIONS

The following conclusions are drawn from the numerical results obtained.

- Centrifugal forces increase the values of principal stresses at the inner surface of ceramic discs.

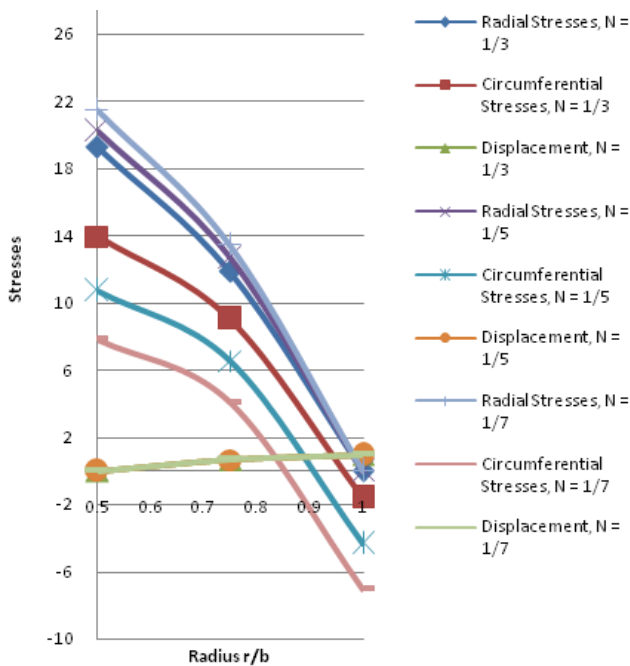


Figure 2. Creep stresses and displacement in BaTiO₃ along the radius ratios $R = r/b$ at $\Omega^2 = 50$.

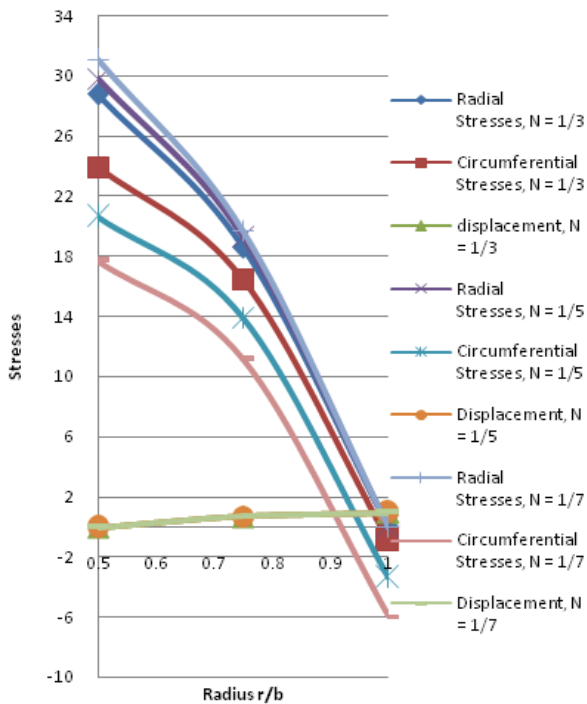


Figure 3. Creep stresses and displacement in PZT-5H along the radius ratios $R = r/b$ at $\Omega^2 = 100$.

- Strains are maximal at inner surface and diminish toward the outer surface. The rise in strains with increase in centrifugal forces infers to the fact that the disc will tend to fracture at the bore adjoining the inclusion when subjected to higher forces. Stresses at various radii ratios are given in the numerical results to check for points where ceramic discs will no longer sustain the centrifugal forces.

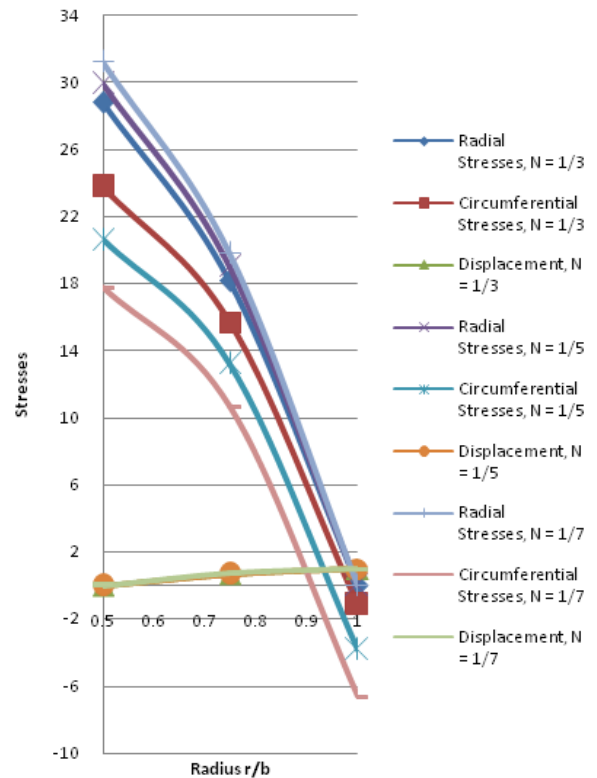


Figure 4. Creep stresses and displacement in BaTiO₃ along the radius ratios $R = r/b$ at $\Omega^2 = 100$.

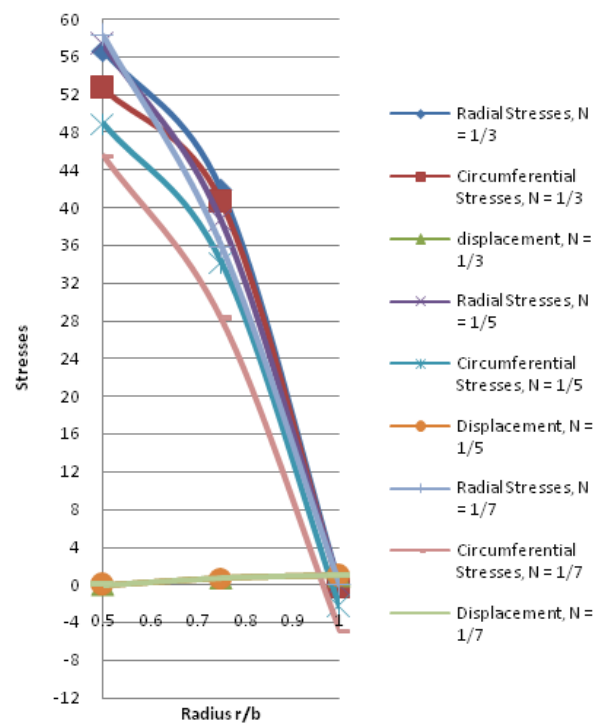


Figure 5. Creep stresses and displacement in PZT-5H along the radius ratios $R = r/b$ at $\Omega^2 = 150$.

- It is primarily concluded that it is mandatory to reinforce such type of ceramic discs with another material in the region close to the bore, so as to increase the stress withstanding capacity of the disc, thereby leading to a safer design.

The paper provides the scope for the development of functionally graded ceramic discs, reinforced close to the inner radius.

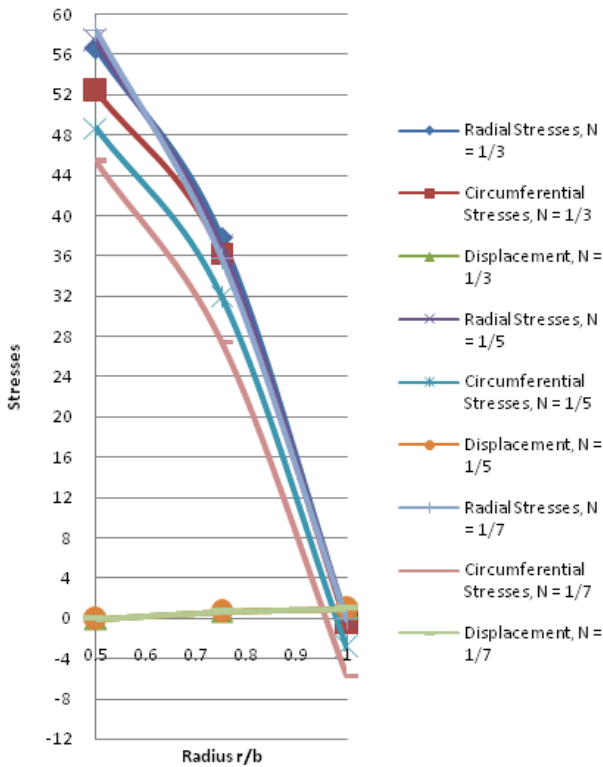


Figure 6. Creep stresses and displacement in BaTiO₃ along the radius ratios $R = r/b$ at $\Omega^2 = 150$.

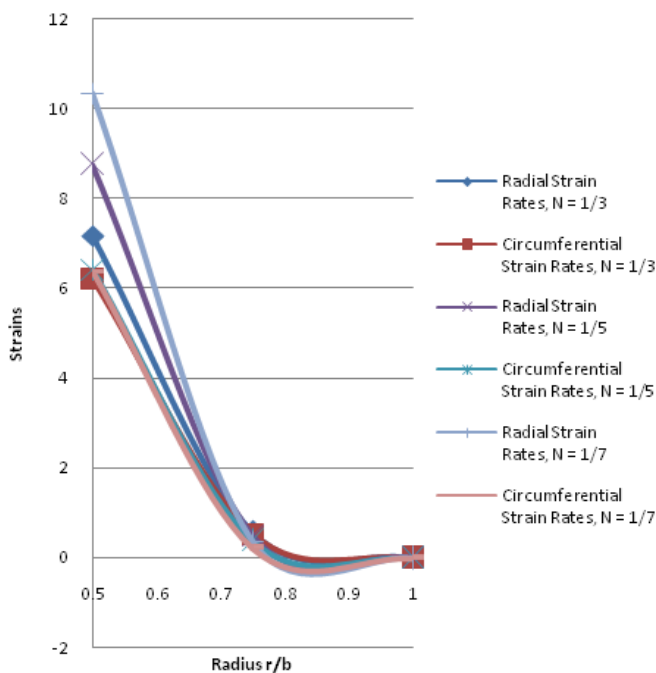


Figure 7. Creep strain rates in PZT-5H along the radius ratios $R = r/b$ at $\Omega^2 = 50$.

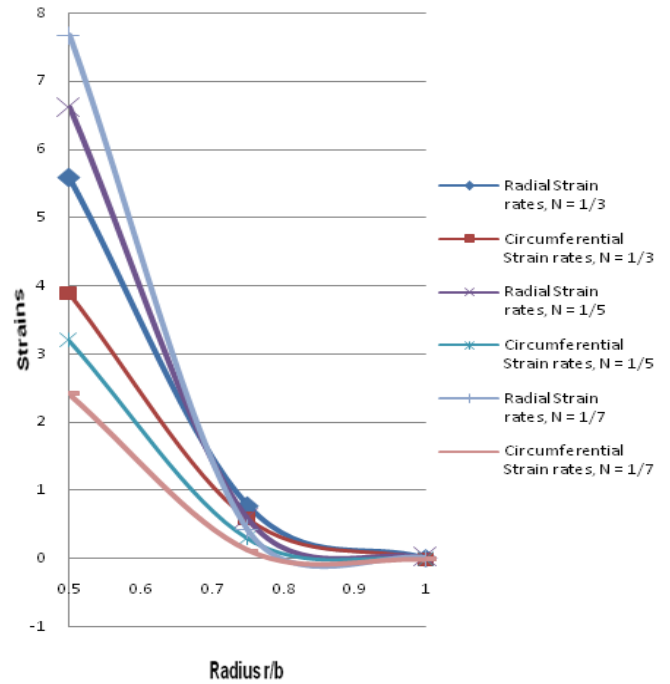


Figure 8. Creep strain rates in BaTiO₃ along the radius ratios $R = r/b$ at $\Omega^2 = 50$.

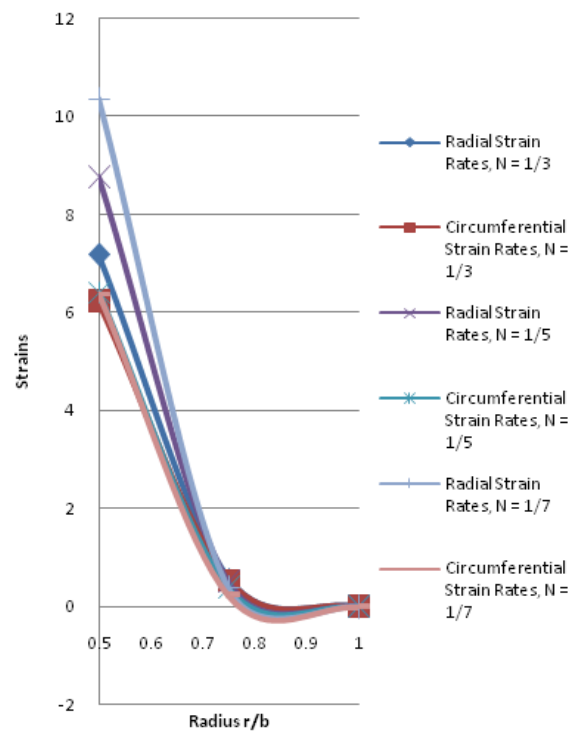


Figure 9. Creep strain rates in PZT-5H along the radius ratios $R = r/b$ at $\Omega^2 = 100$.

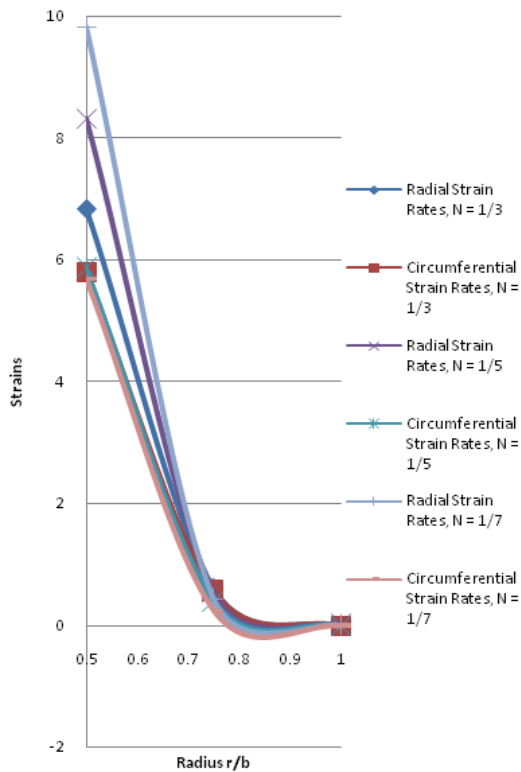


Figure 10. Creep strain rates in BaTiO₃ along the radius ratios $R = r/b$ at $\Omega^2 = 100$.

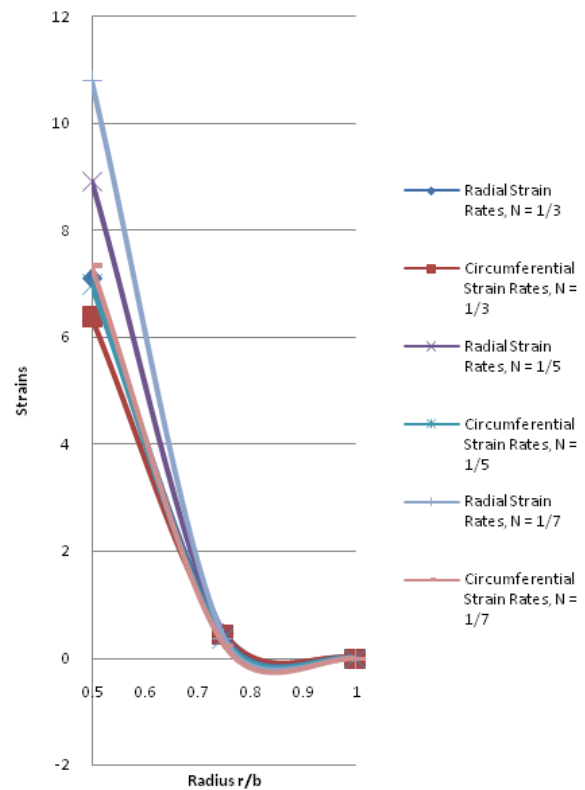


Figure 12. Creep strain rates in BaTiO₃ along the radius ratios $R = r/b$ at $\Omega^2 = 150$.

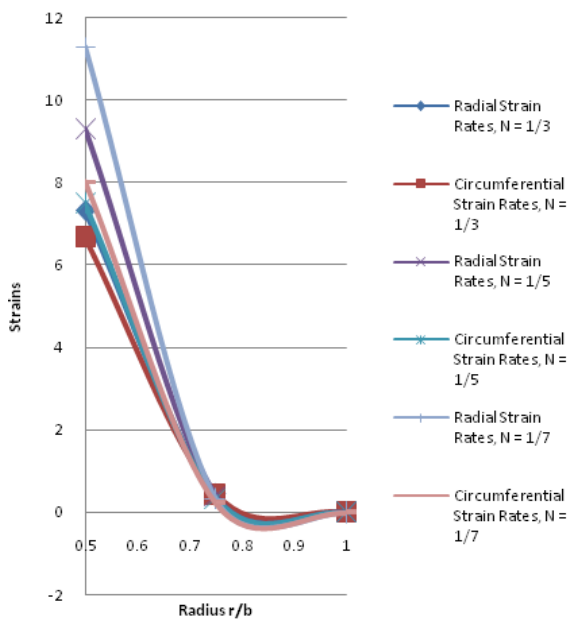


Figure 11. Creep strain rates in PZT-5H along the radius ratios $R = r/b$ at $\Omega^2 = 150$.

REFERENCES

1. Amenzade, Yu.A., Theory of Elasticity, MIR Publishers, Moscow, 1979, pp.123-125.
2. Chakrabarty, J., Theory of Plasticity, McGraw-Hill, New York, 1987.
3. Fung, Y.C. (Ed.), Foundations of Solid Mechanics, Englewood Cliffs, N.J. Prentice-Hall, 1965.
4. Gupta, S.K., Thakur, P. (2007), Creep transition in a thin rotating disc with rigid inclusion, Defence Sci. J., 57(2):185-195.
5. Gupta, S.K., Thakur, P. (2007), Thermo elastic-plastic transition in a thin rotating disc with inclusion, Therm. Sci. 11(1): 103-118. doi: 10.2298/TSCI0701103G
6. Guven, U. (1999), Elastic-plastic rotating disk with rigid inclusion, Mech. Struct. Mach. 27(1): 117-128. doi: 10.1080/08905459908915691
7. Ding, H.J., Chen, W.Q., Zhang, L., Elasticity of Transversely Isotropic Materials (Series: Solid Mechanics and Its Applications), Springer, Dordrecht, Netherlands, 2006. doi: 10.1007/1-4020-4034-2
8. Hetnarski R., Ignaczak, J., Mathematical Theory of Elasticity, 1st Ed., Taylor and Francis, 2003.
9. Kraus, H., Creep Analysis, John Wiley & Sons, Inc., New York, 1980. ISBN 0471062553
10. Odqvist, F.K.G., Mathematical Theory of Creep and Creep Rupture, Clarendon Press, Oxford, 1974.
11. Royer, D., Dieulesaint, E., Elastic Waves in Solids I: Free and Guided Propagation, Springer-Verlag, Berlin, 2000.
12. Seth, B.R. (1962), Transition theory of elastic-plastic deformation, creep and relaxation, Nature, 195: 896-897. doi:10.1038/195896a0
13. Seth, B.R. (1966), Measure concept in mechanics, Int. J Non-linear Mech., 1(1): 35-40. doi: 10.1016/0020-7462(66)90016-3
14. Shahi, S., Singh, S.B., Thakur, P. (2019), Modeling creep parameter in rotating discs with rigid shaft exhibiting transversely

- isotropic and isotropic material behavior*, J Emerg. Technol. Innov. Res. 6(1): 387-395.
15. Shahi, S., Singh, S.B., Kumar, P. (2021), *Mathematical modeling of elastic plastic transitional stresses in CNT-GS based hybrid nanocomposite thin walled spherical pressure vessels*, IOP Conf. Ser.: Mater. Sci. Eng. 1033: 012058. doi: 10.1088/1757-899X/1033/1/012058
16. Sharma, S., Sahni, M. (2009), *Elastic-plastic transition of transversely isotropic thin rotating disc*, Contemp. Eng. Sci. 2(9): 433-440.
17. Sokolnikoff, I.S., *Mathematical Theory of Elasticity*, 2nd Ed., McGraw-Hill Inc., New York, 1953.
18. Thakur, P., Kaur, J., Singh, S.B. (2016), *Thermal creep transition stresses and strain rates in a circular disc with shaft having variable density*, Eng. Comput. 33(3): 698-712. doi: 10.1108/EC-05-2015-0110
19. Thakur, P., Gupta, N., Singh, S.B. (2017), *Creep strain rates analysis in cylinder under temperature gradient materials by using Seth's theory*, Eng. Comput. 34(3): 1020-1030. doi: 10.1108/EC-05-2016-0159
20. Thakur, P., Sethi, M., Shahi, S., et al. (2018), *Exact solution of rotating disc with shaft problem in the elastoplastic state of stress having variable density and thickness*, Struct. Integr. Life, 18(2): 128-134.
21. Thakur, P., Shahi, S., Gupta, N., Singh, S.B. (2017), *Effect of mechanical load and thickness profile on creep in a rotating disc by using Seth's transition theory*, AIP Conf. Proc., Amer. Inst. of Physics, USA, 1859(1): 020024. doi.org/10.1063/1.4990177
22. Thakur, P., Shahi, S., Singh, S.B., Sethi, M. (2019), *Elastic-plastic stress concentrations in orthotropic composite spherical shells subjected to internal pressure*, Struct. Integr. Life, 19(2): 73-77.
23. Timoshenko, S.P., Goodier, J.N., *Theory of Elasticity*, Third Ed., Mc Graw-Hill Book Co. New York, London, 1951.
24. Todhunter, I., Pearson, K., *A History of the Theory of Elasticity and of the Strength of Materials*, 2, Cambridge University Press, 1893.
25. Wang, H., Cao, W. (2002), *Determination of full set material constants of piezoceramics from phase velocities*, J Appl. Phys. 92(8): 4578-4583. doi: 10.1063/1.1505998
26. You, L.H., Zhang, J.J., You, X.Y. (2005), *Elastic analysis of internally pressurized thick-walled spherical pressure vessels of functionally graded materials*, Int. J Press. Ves. Piping, 82 (5): 347-354. doi: 10.1016%2Fj.ijpvp.2004.11.001

© 2024 The Author. Structural Integrity and Life. Published by DIVK (The Society for Structural Integrity and Life 'Prof. Dr Stojan Sedmak') (<http://divk.inovacionicentar.rs/ivk/home.html>). This is an open access article distributed under the terms and conditions of the Creative Commons Attribution-NonCommercial-NoDerivatives 4.0 International License